JBC RESEARCH ARTICLE

PrkA is an ATP-dependent protease that regulates sporulation in *Bacillus subtilis*

Received for publication, February 10, 2022, and in revised form, August 15, 2022 Published, Papers in Press, August 28, 2022,
https://doi.org/10.1016/j.jbc.2022.102436

Ao Zhang[1], **Régine Lebrun**[2], **Leon Espinosa**[1], **Anne Galinier**[1], **and Frédérique Pompeo**[1,*]

From the [1]*Laboratoire de Chimie Bactérienne, UMR 7283, IMM, CNRS, and* [2]*Plateforme Protéomique de l'IMM, Marseille Protéomique (MaP), CNRS FR 3479, Aix-Marseille Université, Marseille, France*

Edited by Chris Whitfield

In *Bacillus subtilis*, sporulation is a sequential and highly regulated process. Phosphorylation events by histidine kinases are key points in the phosphorelay that initiates sporulation, but serine/threonine protein kinases also play important auxiliary roles in this regulation. PrkA has been proposed to be a serine protein kinase expressed during the initiation of sporulation and involved in this differentiation process. Additionally, the role of PrkA in sporulation has been previously proposed to be mediated *via* the transition phase regulator ScoC, which in turn regulates the transcriptional factor σ^K and its regulon. However, the kinase activity of PrkA has not been clearly demonstrated, and neither its autophosphorylation nor phosphorylated substrates have been unambiguously established in *B. subtilis*. We demonstrated here that PrkA regulation of ScoC is likely indirect. Following bioinformatic homology searches, we revealed sequence similarities of PrkA with the ATPases associated with diverse cellular activities ATP-dependent Lon protease family. Here, we showed that PrkA is indeed able to hydrolyze α-casein, an exogenous substrate of Lon proteases, in an ATP-dependent manner. We also showed that this ATP-dependent protease activity is essential for PrkA function in sporulation since mutation in the Walker A motif leads to a sporulation defect. Furthermore, we found that PrkA protease activity is tightly regulated by phosphorylation events involving one of the Ser/Thr protein kinases of *B. subtilis*, PrkC. Taken together, our results clarify the key role of PrkA in the complex process of *B. subtilis* sporulation.

Bacillus subtilis is the model organism for gram-positive sporulating bacteria. Sporulation allows bacteria to survive nutritional stress or harsh environmental conditions like heat, chemicals, or UV exposure (1, 2). These dormant cells are able to germinate and to reinitiate growth rapidly in response to environmental signals (3) like nutrients, L-alanine, or muropeptides. Sporulation is well regulated and orchestrated by a series of protein phosphorylation events and changes in genes expression controlled by sequential sigma factors (σ^E, σ^F, σ^G, and σ^K) (4, 5). In *B. subtilis*, these regulations are carried out by two component systems; five histidine kinases (KinA-KinE) are sensing the environmental changes and initiate sporulation by phosphorylating the transcriptional master regulator Spo0A *via* the phosphotransferases Spo0F and Spo0B (6). Active Spo0A∼P can then directly regulate the expression of numerous genes including those necessary to activate sporulation (7). Spore germination is initiated by germinant receptors embedded in the spore inner membrane and able to sense low amounts of germinants to activate a still poorly understood signal transduction pathway (8) leading to a three phases revival process. However, sporulation and germination have been shown to be also regulated by some phosphorylation events that are carried out by Ser/Thr protein kinases (STPKs) of the Hanks family like PrkA, PrkC, and YabT (9). In this paper, we will focus on PrkA protein that is conserved in several sporulating bacteria. The *prkA* gene is expressed during sporulation and controlled by the σ^E transcription factor. The deletion of *prkA* leads to a reduction in the number of spores and in an important sporulation defect (10). It has also been shown that PrkA was involved in the synthesis of the σ^K transcription factor and its downstream target genes, by inhibiting, directly or indirectly, the transcriptional regulator ScoC (11). Indeed, the authors demonstrated that *prkA* deletion led to a decrease of σ^K expression that finally caused a sporulation defect, both being complemented by an elevated level of σ^K. They further observed that ScoC negatively regulated the expression of σ^K, and this regulation was epistatic to PrkA in sporulation. On the other hand, PrkA from *B. subtilis* was initially referred as a potential protein kinase with a N-terminal domain related to the superfamily of ATPases associated with diverse cellular activities (AAA+) and a C-terminal domain with distant homology to (cAMP)-dependent protein kinases (12, 13). However, despite the first paper in 1996 describing the ability of PrkA to phosphorylate an unidentified 60 kDa protein from crude extract on Ser residue, no characterization of PrkA as a protein kinase has been demonstrated so far. Furthermore, no PrkA autophosphorylation was detected which was surprising since STPKs generally need to be autophosphorylated to be active. Recently, a homologous protein from *Escherichia coli*, YeaG, has been shown to be indeed a kinase that autophosphorylates (14) and phosphorylates AceA, the isocitrate lyase involved in the glyoxylic cycle, in the presence of malate (15), but this catalytic pathway is missing in *B. subtilis*.

* For correspondence: Frédérique Pompeo, fpompeo@imm.cnrs.fr.

In this paper, we reinvestigated the enzymatic properties of PrkA from *B. subtilis*. Despite our efforts, we did not observe an autophosphorylation or a kinase activity for this protein. However, new bioinformatic homology searches revealed sequence similarities between Lon proteases and PrkA. Lon proteases are enzymes belonging to the (AAA+) ATP-dependent protease family (16, 17) whose activity depends on ATP hydrolysis; they are generally involved in protein quality control or in the degradation of important cellular regulators (18, 19). We showed that PrkA is able to hydrolyze α-casein, an exogenous substrate of Lon proteases, in the presence of ATP and that this activity is regulated by phosphorylation by the Ser/Thr kinase PrkC. In addition, the ATP-dependent protease activity of PrkA is needed for its function in the control of sporulation initiation in *B. subtilis*. If the control of sporulation by PrkA is mediated *via* the ScoC regulator as previously proposed (11), our data suggest that it should be by an indirect way.

Results

PrkA is able to bind and hydrolyze ATP

PrkA was first referred as a potential protein kinase necessary for *B. subtilis* sporulation with a N-terminal domain related to the superfamily of (AAA+) ATPases and a C-terminal domain with distant homology to (cAMP)-dependent protein kinases (12). This suggests that PrkA potentially possesses two distinct ATP binding motifs, one located in the N-terminal domain for the ATPase activity and another one located in the C-terminal domain for kinase activity. ATPase enzymes possess in their sequence a Walker A motif known to be involved in ATP binding and hydrolysis (20, 21). A Walker A motif was easily identified in the N-terminal sequence of PrkA, but the P-loop motif usually involved in ATP binding for Hanks kinases seems to be degenerated in the C-terminal part of PrkA (see alignment in Fig. S1). The biochemical characterization of PrkA enzyme led us to firstly test the role of Walker A motif. We thus mutated the conserved residue Lys108 to Ala and investigated the ATP binding ability of WT and PrkA-K108A. Using proteolytic digestion (Fig. 1*A*), we observed different patterns of proteolysis depending on the presence or on the absence of ATP. This observation indicated that ATP binding induces PrkA conformational changes that protect it from GluC proteolytic digestion. By contrast, for PrkA-K108A, we obtained the same pattern of degradation by GluC with or without ATP (Fig. 1*A*). This suggests that either ATP can no longer bind to PrkA-K108A or, less probably, ATP binds to PrkA-K108A but cannot induce conformational changes in this mutated protein. To validate these data and to determine the binding kinetic parameters, we used thermal shift assays (Fig. 1*B*). We showed that PrkA binds ATP with an apparent Kd = 0.25 mM, but binding of ATP to PrkA-K108A was too low to accurately estimate the affinity. Moreover, the maximum temperature difference was barely measurable for

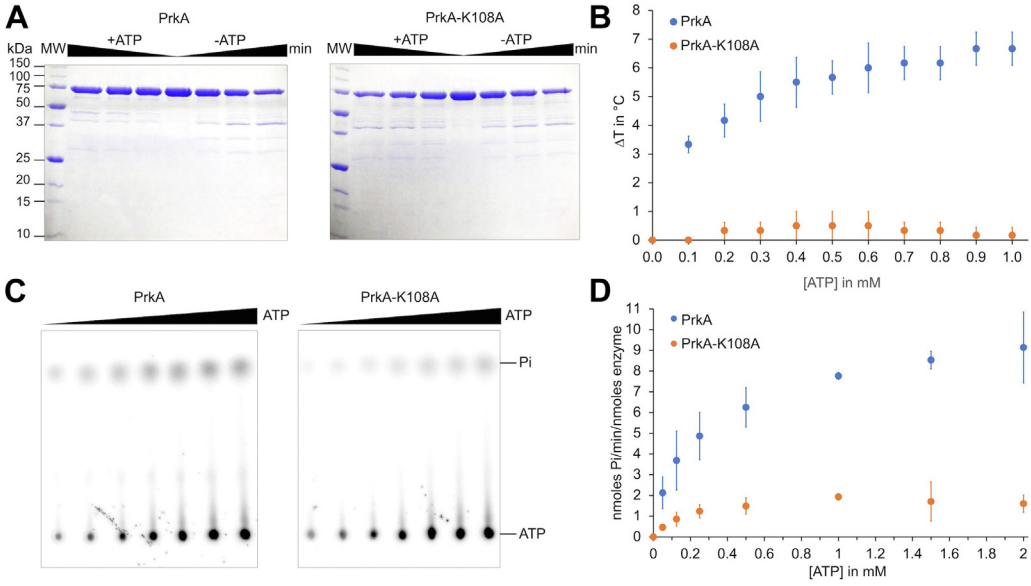

Figure 1. The Walker A motif of PrkA is important for ATP binding and hydrolysis. *A*, Coomassie-stained SDS-PAGE of PrkA (*left gel*) or PrkA-K108A (*right gel*) partial proteolysis profiles. PrkA proteins were incubated with endoproteinase Glu-C in the absence or in the presence of 1 mM ATP for 0, 15, or 30 min at 37 °C. The digestion profiles were assessed by electrophoresis in 12.5% SDS-PAGE. *B*, thermal shift assay in the presence of increasing amounts of ATP and 10 mM $MgCl_2$. Assays were performed with PrkA and PrkA-K108A in the presence of increasing concentrations of ligand (0–1 mM). The difference of temperature [the shift of melting temperature of the protein (Tm) induced by the presence of ligand] was plotted against the concentration of ATP. Each experiment was reproduced at least in triplicate, and the standard deviations are represented by the error bars. *C*, ATPase activity assays using thin layer chromatography. Increasing concentrations of 1 μCi [γ-^{33}P] ATP (0–2 mM) were incubated for 2 min at 37 °C with 8 μM of PrkA or PrkA-K108A and 5 mM $MgCl_2$. ATP hydrolysis was stopped by addition of formic acid. Residual ATP and released Pi were separated by TLC using PEI-cellulose F plates in formic acid and LiCl buffer. Plates were then dried and exposed to autoradiography. *D*, quantification of ATPase activity. Assays were performed as described in (*C*). The amount of Pi released was estimated by using ImageJ software. The values obtained for the negative control (without PrkA) were subtracted from those of the tested proteins. The specific activity of each protein (nmol of Pi released/nmol of enzyme/min) was plotted against the concentration of ATP used. Each experiment was reproduced at least in triplicate and the standard deviations are represented by the error bars. TLC, thin layer chromatography.

PrkA-K108A (ΔT_{max} estimated = 0.35 °C) compared to 9.38 °C for WT-PrkA showing that the binding of ATP was highly affected by the replacement of lysine to alanine. This confirmed that the Walker A motif of PrkA is indeed involved in ATP binding and is probably the only motif responsible for binding of this nucleotide in the protein. This result was not surprising since the potential C-terminal P-loop appears degenerated. We then hypothesized that PrkA was capable of hydrolyzing ATP and that Walker A motif was involved in this enzymatic activity. We firstly determined the appropriate experimental conditions of Michaelis–Menten kinetics using thin layer chromatography and radioactive ATP (Fig. S2). Although it is challenging to get a linear fit with this assay (Fig. S2), we chose the best conditions to test PrkA ATPase activity as well as that of the PrkA-K108A mutant protein; we observed that the intensity of radioactive spot corresponding to the Pi released was increasing with the amount of PrkA whereas it increased a lot less with the addition of PrkA-K108A (Fig. 1*C*). These results proved that PrkA binds and hydrolyzes ATP *via* its Walker A motif. The enzymatic parameters were determined (Fig. 1*D*), and we observed that PrkA hydrolyzes ATP with a Kcat = 12.88 ± 0.63 nmol/min/nmol of enzyme and a Km = 0.53 ± 0.09 mM. In addition, whereas the Km value is moderately affected (Km = 0.13 ± 0.03 mM), the Kcat is 7 times lower (Kcat = 1.80 ± 0.15 nmol/min/nmol of enzyme) for PrkA-K108A, supporting that the Walker A motif is essential for PrkA to bind and hydrolyze ATP (Fig. 1*D*).

PrkA is not autophosphorylated nor a kinase

Because PrkA was proposed to be a protein kinase containing a C-terminal domain with distant homology to (cAMP)-dependent protein kinases and that its *E. coli* homologue YeaG (Fig. S1) is a kinase, we decided to test PrkA autophosphorylation and kinase activity in several conditions using radioactive ATP. Comparing the autoradiogram presented in Figure 2 (left) to the corresponding Coomassie-stained SDS-PAGE gel (Fig. 2, right), we can observe that PrkA alone is not able to autophosphorylate (lane 4) nor is it able to phosphorylate the exogenous myelin basic protein substrate often phosphorylated by STPK (22) (lane 1) nor any protein of a *B. subtilis* crude extract from bacteria grown until late stationary phase in sporulation medium (lane 2). When the same conditions (Tris/HCl buffer at pH = 7.5, 2.5 mM $MgCl_2$, 5 mM ATP) were used for the catalytic domain of the STPK PrkC, PrkCc, a strong autophosphorylation signal was detected (Fig. 2, lane 5). Other conditions like addition of $MnCl_2$, cAMP, or pyruvate were tested (data not shown), but despite our effort, no signal was detected. Therefore, we have not been able so far to show an autophosphorylation or a kinase activity for PrkA. In addition, our previous experiments of ATP binding to PrkA did not provide any evidence that PrkA possesses an ATP-binding site located in its C-terminal domain. We conclude that PrkA binds ATP *via* its Walker A motif located in its N-terminal domain and is therefore an ATPase but does not appear to be a kinase as initially assumed.

The ATPase activity is necessary for B. subtilis *sporulation*

To test the importance of PrkA ATPase activity on its cellular role, we constructed *prkA*-deleted strains producing from an ectopic site, the WT-PrkA (strain SG611, Table 1) or the mutated PrkA-K108A protein (strain SG613) and checked by Western blot using PrkA antibodies that WT-PrkA and PrkA-K108A were produced at the same level as the native protein (Fig. S3). We then compared the sporulation efficiency (Fig. 3*A*, light gray boxes) of these new strains to that of the WT and the deleted *prkA* (SG605) strains (Table 1) by the heat-killing method. As expected, the deleted strain SG605 was

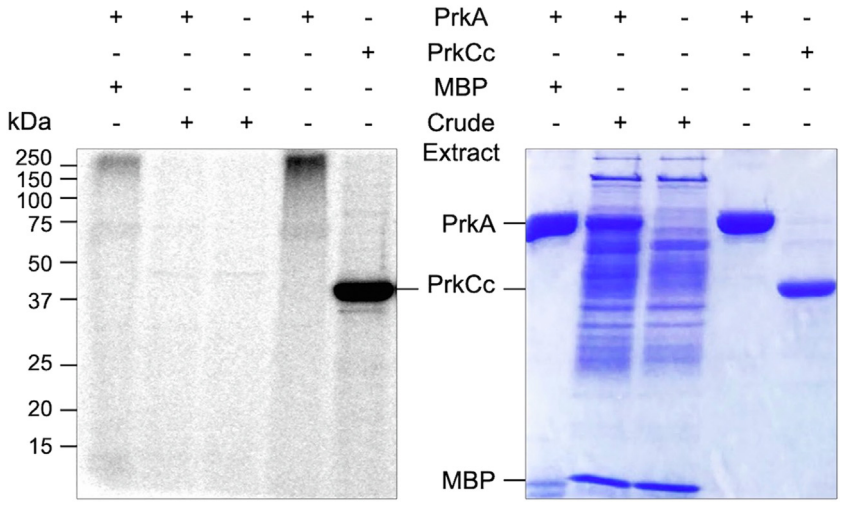

Figure 2. PrkA does not autophosphorylate and is not a kinase. Autoradiogram (*left*) and respective Coomassie-stained gel (*right*) for PrkA phosphorylation activity test. PrkA was incubated for 1 h at 37 °C alone (lane 4) or with MBP (lane 1) or *B. subtilis* crude extract from a stationary phase culture in DSM medium (lane 2) in a reaction mixture containing 10 mM Tris/HCl, pH 7.5, 2.5 mM $MgCl_2$ and 0.5 mM [γ-^{33}P] ATP (1 μCi). Controls corresponding to *B. subtilis* crude extract without PrkA (lane 3) or the catalytical domain of PrkC instead of PrkA (lane 5) were assessed in parallel. The phosphorylation reaction was stopped by adding 5× SDS-loading buffer to the reaction mixtures before 12.5% SDS-PAGE analysis. Gels were then dried and exposed to autoradiography. DSM, Difco sporulation medium.

Table 1
***B. subtilis* strains and plasmids used in this work**

Strain/plasmid	Relevant characteristics	Source/reference
Bacillus subtilis strains		
WT168	*trpC2*	lab collection
SG605	*trpC2 prkA::cm*	This work
SG611	*trpC2 prkA::cm; amyE::Pspac-prkA*	This work
SG613	*trpC2 prkA::cm; amyE::Pspac-prkA-K108A*	This work
SG935	*trpC2 prkA::cm; amyE::Pspac-prkA-T217A*	This work
SG936	*trpC2 prkA::cm; amyE::Pspac-prkA-T217E*	This work
SG940	*trpC2 prkA::cm; amyE::Pspac-prkA-T217A-S219A*	This work
SG941	*trpC2 prkA::cm; amyE::Pspac-prkA-T217E-S219E*	This work
Plasmids		
pET21a-*prkA*		This work
pET21a-*scoC*		This work
pET21a-*prkA-K108A*		This work
pET21a-*prkA-T217A*		This work
pET21a-*prkA-T217D*		This work
pET21a-*prkA-T217E*		This work
pET21a-*prkA-S219A*		This work
pET21a-*prkA-S219D*		This work
pET21a-*prkA-S219E*		This work
pET21a-*prkA-T217A-S219A*		This work
pET21a-*prkA-T217D-S219D*		This work
pET21a-*prkA-T217E-S219E*		This work
pAC7-*prkA*		This work
pAC7-*prkA-K108A*		This work
pAC7-*prkA-T217A*		This work
pAC7-*prkA-T217E*		This work
pAC7-*prkA-T217A-S219A*		This work
pAC7-*prkA-T217E-S219E*		This work

highly affected in its ability to sporulate (7% compared to 67% for the WT), and this phenotype was complemented by expression of *prkA* in the SG611 strain (58% of sporulation). We were then able to confirm that the ATP-binding capacity of PrkA, and therefore its activity, was essential for its role in sporulation since we observed that the mutated strain SG613 producing PrkA-K108A was only able to sporulate with a rate of 13% similar to that of the deleted strain. As the method by heat-killing of the nonsporulating cells used in the previous sporulation test implies that the spores are able to germinate,

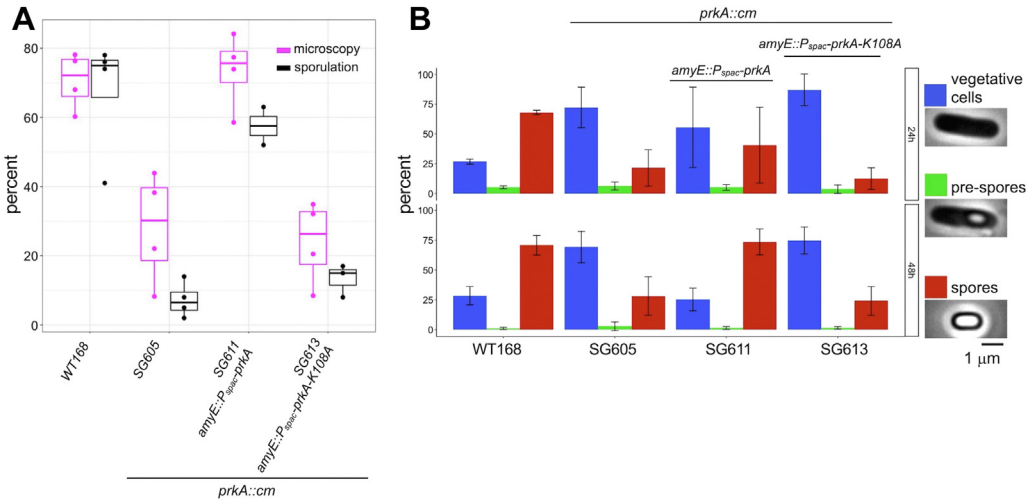

Figure 3. Sporulation efficiency and morphological analysis of wildtype and mutant *B. subtilis* strains. *A*, quantification by two approaches of sporulation efficiency after 48 h in DSM for the WT, SG605(*prkA::cm*), SG611(*prkA::cm; amyE::Pspac-prkA*), and SG613(*prkA::cm; amyE::Pspac-prkA-K108A*) strains. The *black boxplots* represent the results of 2 to 4 biological replicates of sporulation rate evaluation based on the number of heat-resistant (80 °C for 20 min) CFUs (the *black line* represents the median of the group and the *dots* each biological replicate). *Magenta boxplots* represent the quantification of the ratio of spores over the total number of cells in at least 20 microscopy fields for each strain (cells per group > 4000, from four independent biological replicates represented as *dots*). The Wilcoxon statistical test yielded nonsignificant differences between these two methods even if the image-based method shows slightly higher rates. *B*, cells classification from microscopy images. Microscopy images in phase contrast modality allow to easily classify the cells based on the maximum of intensity and the cell length: long cells with low intensity are the vegetative cells (*blue*), long cells with high intensity are the prespores (*green*), and small cells with high intensity are the spores (*red*). All cellular measurements were obtained automatically with MicrobeJ software. The number of cells in each type for each strain was reported here as percentages in columns at 24 and 48 h in DSM. The error bars represent the standard deviation over the four independent biological replicates, and the number of cells per group for each replicate exceeds 4000. A Wilcoxon test performed between biological replicates shows that the WT168 strain yields significant differences ($p < 0.05$) compared with mutants SG605 and SG613 (excepted for SG613 spores at 24 h where $p = 0.0571$); in contrast, compared with SG611, the test yields no significant differences. There are no differences between SG605 and SG613. CFU, colony forming unit; DSM, Difco sporulation medium.

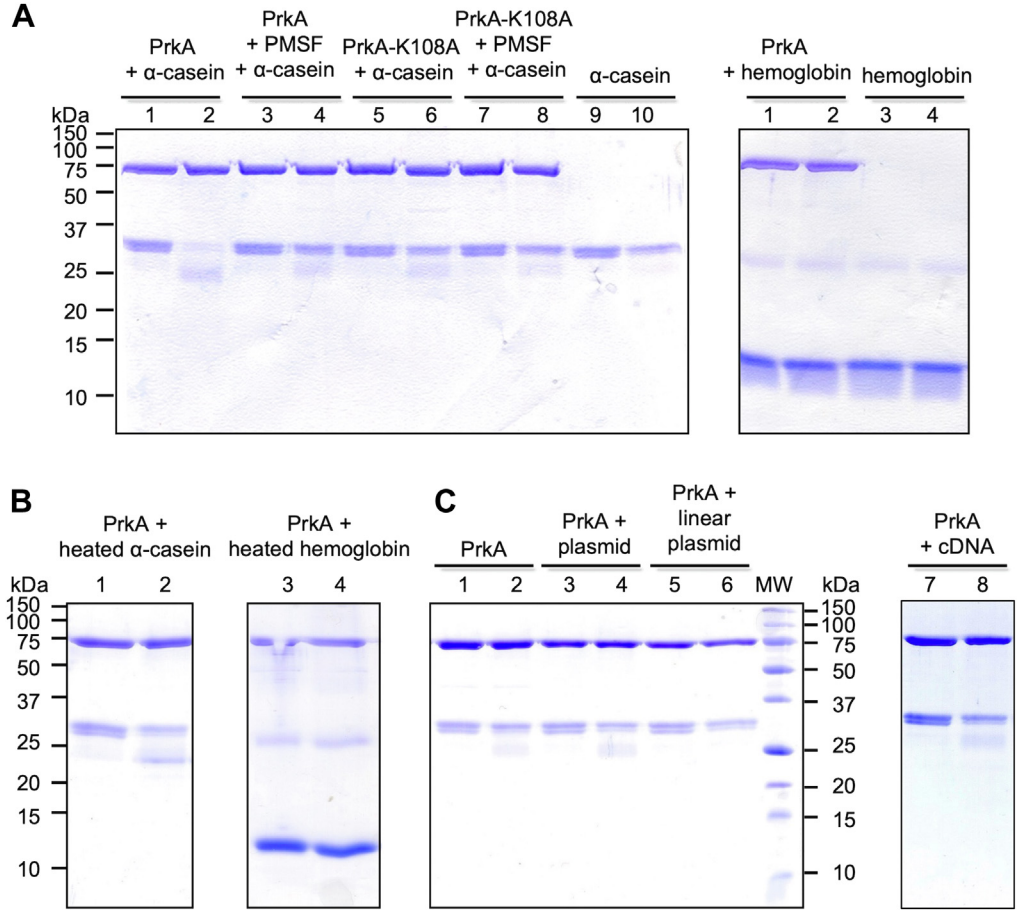

Figure 4. PrkA possesses a protease activity. Coomassie-stained SDS-PAGE of α-casein and hemoglobin proteolysis. *A*, α-casein (*left gel*) or hemoglobin (*right gel*) proteolytic digestion by PrkA (or PrkA-K108A, *left gel* - lanes 5–8) was assessed by incubation at 37 °C for 0 (odd-numbered columns) or 24 h (even-numbered columns) in the presence of 1 mM $MgCl_2$ and 1 mM ATP. Inhibition of PrkA (or PrkA-K108A) protease activity was tested by addition of 1 mM PMSF (lanes 3, 4, and 7, 8 respectively). *B*, proteolytic digestion by PrkA was performed as described above except that protein substrates were previously heated for 10 min at 85 °C. *C*, Coomassie-stained SDS-PAGE of α-casein proteolysis in the presence of DNA. Proteolytic digestion by PrkA was performed as described above except that 20 ng of circular or linearized plasmids or 120 ng of cDNA were added to the reaction. PMSF, phenylmethylsulfonyl fluoride.

we also quantified the number of spores formed after 24 and 48 h in Difco sporulation medium (DSM) medium by microscopy (Fig. 3*A* magenta boxplots and Fig. 3*B*). The advantage of the microscopic analysis is that it also allows us to count the number of prespores in addition to spores and vegetative cells (Fig. 3*B*). Thus, by comparing the percentages of each type of cells at 24 and 48 h, we can conclude that the absence of PrkA (strain SG605) leads to a reduction of the total number of spores formed (Fig. 3*B*). This defect is complemented at a spore level equivalent to that of the WT strain for SG611 producing the WT protein but not for SG613 producing the inactive protein. Moreover, the final quantification at 48 h (Fig. 3*A*) gave approximately the same rates of sporulation for all the tested strains with the two methods confirming that the ability of the cells to sporulate is actually affected in the absence of PrkA activity and not the ability of the spores to germinate. Altogether, these data demonstrated that PrkA binds and hydrolyzes ATP thanks to its Walker A motif and that the ATP-dependent activity of PrkA is necessary to *B. subtilis* cells for efficient sporulation.

PrkA is an AAA+ ATP-dependent protease

In order to better understand the function of PrkA, we looked for proteins with sequence similarities and identified by BLAST some Lon proteases from several bacterial species (Fig. S4). The resulting alignment of PrkA and YeaG sequences with those of four bacterial Lon proteases showed a good overall homology, and several amino acids from conserved regions are strictly identical or strongly similar in PrkA sequence. However, we noticed that, in this alignment, the position of the Walker A motif of Lon and of PrkA is different. This new information led us to test PrkA for a protease activity (Figs. 4*A* and S5). Using known exogenous substrates of Lon enzymes like α-casein and hemoglobin, we were able to demonstrate that PrkA was indeed a protease able to digest α-casein (left gel, lanes 1 and 2) but not hemoglobin (right gel, lanes 1 and 2) in the presence of ATP within 24 h at 37 °C. As control, we observed that the proteins alone at 37 °C are stable for 24 h as shown in left gel lanes 9 and 10 and right gel lanes 3 and 4. Since Lon enzymes are often involved in quality control of proteins, we tested if PrkA activity would be increased with

unfolded proteins using these two potential substrates previously heated for 10 min at 85 °C. However, the results were similar for the native or denatured proteins (Fig. 4*B*). We next confirmed the Lon-like protease activity thanks to its specific inhibition by a protease inhibitor, the phenylmethylsulfonyl fluoride (PMSF) (Fig. 4*A*, left gel lanes 3 and 4). Moreover, we showed that ATP hydrolysis was needed for this activity by testing PrkA-K108A which turned out to be an inactive protein as expected (lanes 5 and 6) and with experiments carried out in the absence of ATP (Fig. S6). Some Lon proteases have been described to be regulated by DNA (23); we then tested the addition of circular or linear plasmid or of cDNA in the reaction (Fig. 4*C*), but no effect was detected. Since PrkA protease activity seemed very slow, we excluded the possibility of activity contributed by a contaminant by adding a purification step of PrkA by ion-exchange chromatography and the activity of PrkA remained unchanged (Fig. S7). We therefore demonstrated for the first time that PrkA carries a Lon-like protease activity that is indeed ATP-dependent.

PrkA is phosphorylated by PrkC in vitro

As proteolysis is an irreversible mechanism, protease activities need to be regulated, and Lon proteases activity has been shown to be controlled by several effectors (*e.g.*, DNA, peptides, and metal ions) (23, 24) or posttranslational modifications of the enzymes themselves or of their protein substrates (*e.g.*, phosphorylation, oxidation, ubiquitylation, and pupylation) (25, 26). Recently, Zhou *et al.* demonstrated that Lon protease activity could also be inhibited by phosphorylation on a Ser residue leading to the regulation of bacterial virulence in *Xanthomonas citri*. We then decided to test if PrkA could be regulated by phosphorylation by the PrkC Ser/Thr kinase of *B. subtilis* involved in sporulation and germination. We therefore reproduced α-casein proteolysis kinetics (Fig. 5*A*) with PrkA alone or in the presence of catalytic domain of PrkC, PrkCc, or in the presence of an inactivated kinase domain PrkCc-K40A for 0, 16, 19, or 22 h at 37 °C. Comparing the amount of nondigested α-casein after reaction (Fig. 5*B*), we observed that addition of PrkCc specifically inhibits PrkA protease activity probably through its phosphorylation. In a second step, using a kinase activity test with radioactive ATP, we demonstrated that PrkCc was indeed able to phosphorylate PrkA (Fig. 5*C*, lane 3). Thanks to mass spectrometry analysis, we identified, with high confidence and the best probability site, one peptide of PrkA with one phosphorylation site at T217 (almost 41% phosphorylated) or at S219 (0.5% phosphorylated) (Fig. 5*D*, mass spectrometry proteomics data PXD032931). In order to confirm these results, site-directed mutagenesis was realized on these two residues that were replaced by Ala (phospho-ablative substitution) and Glu or Asp (phospho-mimetic substitutions) as a single or two mutations at the same time. The resulting proteins were tested as PrkC substrates in the presence of radioactive ATP (Fig. 5*C*, lanes 4–9), and we showed that T217 was the major phosphorylation site on PrkA since the radioactive signal was

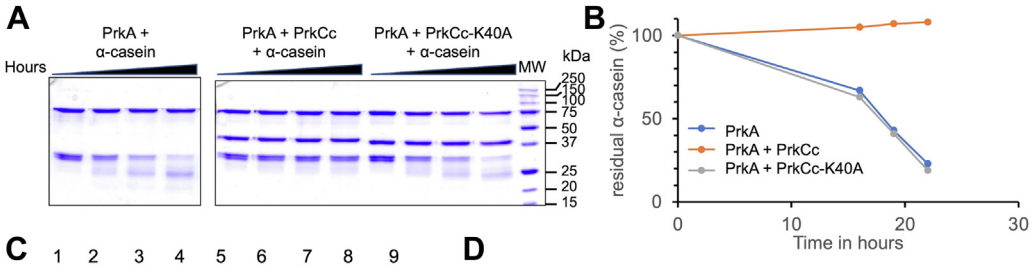

	^{210}SQDIADLTGSIDFSTIAEYGSESDPR^{235}				
	Number of PSM			% Phosphorylation	
Phosphorylation	None	at T217 only	at S219 only	at T217 only	at S219 only
PrkA	119	83	1	40.9	0.5
PrkA-T217E	53	0	0	0	0
PrkA-S219E	45	24	0	34.8	0

Figure 5. PrkA protease activity is regulated by PrkC-dependent phosphorylation. *A*, Coomassie-stained SDS-PAGE of α-casein proteolysis by PrkA. Kinetic of α-casein digestion by PrkA was assessed by incubation at 37 °C for 0, 16, 19, and 24 h in the presence of 1 mM $MgCl_2$ and 1 mM ATP. Inhibition of PrkA protease activity by addition of PrkCc (or inactive PrkCc-K40A) was tested in the same conditions. *B*, graphic presentation of the residual nondigested α-casein estimated (in %) from gels in (*A*) by using ImageJ software plotted against time. *C*, autoradiogram for PrkA phosphorylation by PrkCc. 5 μg of PrkA or the mutated PrkA proteins were incubated for 1 h at 37 °C with 5 μg of PrkCc in Tris/HCl, pH 7.5 buffer containing 2.5 mM $MgCl_2$ and 0.5 mM [γ-^{33}P] ATP (1 μCi). The phosphorylation reaction was stopped by adding 5× SDS-sample buffer to the reaction mixtures before SDS-PAGE analysis. Samples were loaded as follows: lane 1: PrkA, lane 2: PrkCc, lane 3: PrkA+PrkCc, lane 4: PrkA-T217E-S219E+PrkCc, lane 5: PrkA-T217A-S219A+PrkCc, lane 6: PrkA-T217E+PrkCc, lane 7: PrkA-S219E+PrkCc, lane 8: PrkA-T217A+PrkCc, lane 9: PrkA-S219A+PrkCc. Gels were then dried and exposed to autoradiography with FLA5100 Typhoon. *D*, identification of phosphorylated residues by mass spectrometry. PrkA or the mutated PrkA-T217E and PrkA-S219E proteins were phosphorylated by PrkCc in Tris/HCl, pH 7.5 buffer containing 2.5 mM $MgCl_2$ and 0.5 mM ATP then submitted to tryptic digestion for proteomic analysis by nano-LCMS/MS. The mean sequence coverage by tryptic peptides for the three proteins was around 80%, and the only peptide identified with high probability phosphorylation site was ^{210}SQDIADLTGSIDFSTIAEYGSESDPR^{235}. The *red letter* states the alternative position of the phosphorylated residue in the peptide. Phosphorylation at both positions was never observed. The values indicate the number of peptide spectral match (PSM) found in each state (nonphosphorylated, phosphorylated on T217, or phosphorylated on S219) of this peptide, which spectral counting enables the calculation of the phosphorylation ratio: in PrkA, at T217 site, it was almost 41% and 0.5% at S219 site, and in mutant PrkA-S219E, it was almost 35% on T217 site. No phosphorylation was observed on S219 in the PrkA-T217E.

completely lost when T217 was inactivated (Fig. 5*C*, lanes 6 and 8) but remained when S219 (Fig. 5*C*, lanes 7 and 9) was inactivated. As expected, the signal was lost when both sites were mutated (Fig. 5*C*, lanes 4 and 5). We confirmed the previous data by analyzing the phosphorylation status of the mutated proteins PrkA-T217E and PrkA-S219E after reaction with PrkCc by mass spectrometry after Trypsin digestion (Fig. 5*D*, mass spectrometry proteomics data PXD032931). Indeed, we found that for PrkA-T217E, the peptide of interest was found nonphosphorylated whereas for PrkA-S219E, the peptide of interest was found almost 35% phosphorylated on T217. Thus, we demonstrated that PrkA was able to be phosphorylated by PrkC on two sites, T217 and S219, with the threonine being the major site of modification.

The phosphorylation site T217 is important for PrkA function in sporulation

In order to test the role of the two phosphorylated sites of PrkA on its activity, the purified mutated PrkA proteins were firstly tested for their ATP binding ability and their protease activity. TSA experiments showed that both phospho-mimetic and phospho-ablative mutants were still able to bind ATP like the WT protein (Fig. S8). We also noticed that whereas digestion of α-casein after 21 h at 37 °C was similar for all the single mutated proteins (Fig. 6*A*) to that of WT-PrkA, it was significantly less effective for the double phospho-mimetic mutant PrkA-T217D-S219D. These data confirmed that phosphorylation does not prevent ATP fixation but inhibits specifically PrkA protease activity.

We then tested the effect of these mutations on the protease activity of PrkA. We observed that all single mutants were still active even when T217, the major site of phosphorylation, was replaced by a phospho-mimetic residue. However, when both sites T217 and S219 were replaced by phospho-mimetic residues, the inhibition of PrkA was more efficient. To check the importance of these phosphorylation sites on PrkA function *in vivo*, we created new *B. subtilis* strains (Table 1) producing phospho-ablative and phospho-mimetic PrkA proteins. The strains were then tested for their sporulation efficiency (Fig. 6*B*). As observed on the graphic, we found that the strains producing the single-mutated or the double-mutated phospho-ablative proteins PrkA-T217A (SG935) or PrkA-T217A-S219A (SG940) sporulated with the same rate as the WT strain (65 and 59% respectively). By contrast, the strains producing the single-mutated or the double-mutated phospho-mimetic proteins PrkA-T217E (SG936) or PrkA-T217E-S219E (SG941) sporulated like the *prkA*-deleted strain (11 and 6%, respectively). These results indicate that the T217E substitution of the major phosphorylation site is sufficient to inactivate PrkA and to strongly reduce sporulation rate. All together, these data suggest that PrkC regulates the protease activity of PrkA by phosphorylation *in vitro* (Figs. 5*A* and 6*A*) and *in vivo* (Fig. 6*B*). Indeed, we propose that when PrkA is phosphorylated, its protease activity is inhibited; consequently, the sporulation processes is downregulated.

The function of PrkA in sporulation does not involve a direct regulation of ScoC

It has been proposed that PrkA regulates sporulation by inhibiting directly or indirectly the transcriptional regulator ScoC. Indeed, PrkA would inhibit ScoC which in turn negatively regulates the expression of the σ^K transcription factor (11) *via* two different pathways. ScoC has been described to influence σ^E expression by negatively regulating SinI, SinR, and Spo0A that ultimately leads to σ^K inhibition or through a direct inhibition. The expression of σ^K downstream target genes is then affected and finally causes the deficient sporulation. In order to test if PrkA inactivates ScoC by direct proteolysis, we tested if ScoC was a substrate of PrkA in a Lon protease activity test (Fig. 7*A*) and incubated both proteins for 25 h at 37 °C, collecting samples over time. However, no degradation of ScoC was detected in our experiments, suggesting an alternative means of regulation. We therefore tested if PrkA could otherwise modify ScoC function by altering its DNA binding capacity and examined this hypothesis by electrophoretic mobility shift assay (Fig. 7*B*). The band shift observed from lanes 1 and 2 of the gel in Figure 7*B* confirmed that ScoC was able to bind to the upstream region of *epr* gene promoter used as fluorescent DNA template (27). However, addition of increasing amount of PrkA to the reaction mix (lanes 3–8) did not alter the binding affinity of ScoC to DNA. We have thus demonstrated so far that PrkA function in sporulation is linked to its protease activity, but it is unlikely to involve direct interaction with the ScoC regulator.

Discussion

In this work, we showed that despite distant homology with (cAMP)-dependent protein kinases for its C-terminal domain (12) and with the Ser/Thr kinase YeaG from *E. coli* (13–15), no autophosphorylation or kinase activity was detected for PrkA whatever the conditions tested. In addition, our data did not highlight an ATP binding site in the C terminal domain of PrkA. These results, combined with the degeneracy of Hanks-type kinase motifs observed in the PrkA sequence, suggest that this protein may have lost its kinase activity during evolution or may be a pseudokinase. Pseudokinases are abundant in eukaryotes and also present in bacteria. They lack some of the characteristics required for kinase activity (one or more key amino acids or motifs required for efficient ATP coordination or phosphate transfer are usually absent) and are inactive enzymes which can nevertheless be involved in regulatory processes (28, 29). However, we demonstrated for the first time a clear enzymatic activity for the PrkA protein of *B. subtilis*: a protease activity associated to an ATP hydrolysis. Indeed, we unambiguously established that PrkA not only has sequence homologies with Lon proteases but also possesses an ATP-dependent protease activity on the exogenous substrate α-casein. The estimated ATPase specific activity of PrkA (about 13 nmol/min/nmol enzyme) was of the same order of magnitude as those of other ATPases (30, 31). When the Lys108 of the Walker A motif was mutated to Ala, we found that both ATPase and the protease activities were highly

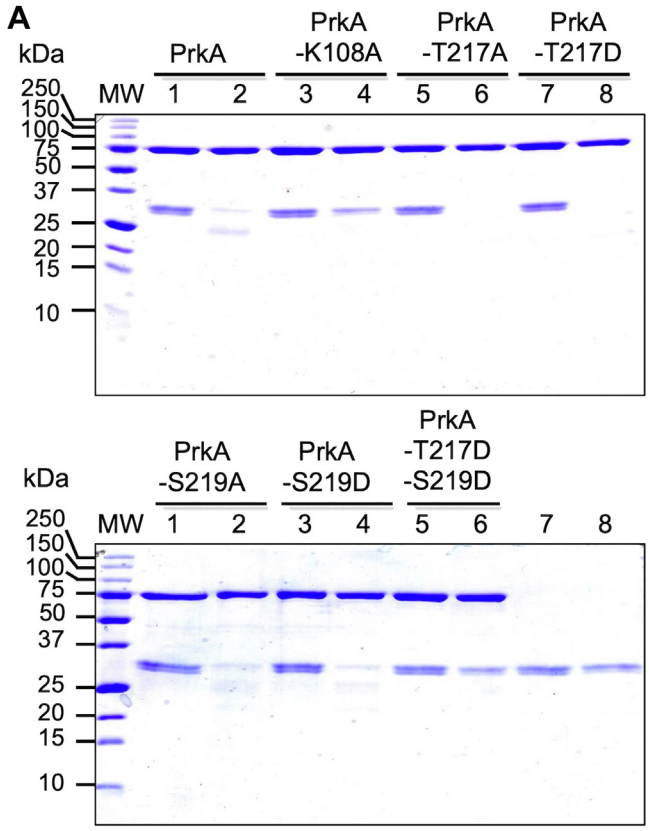

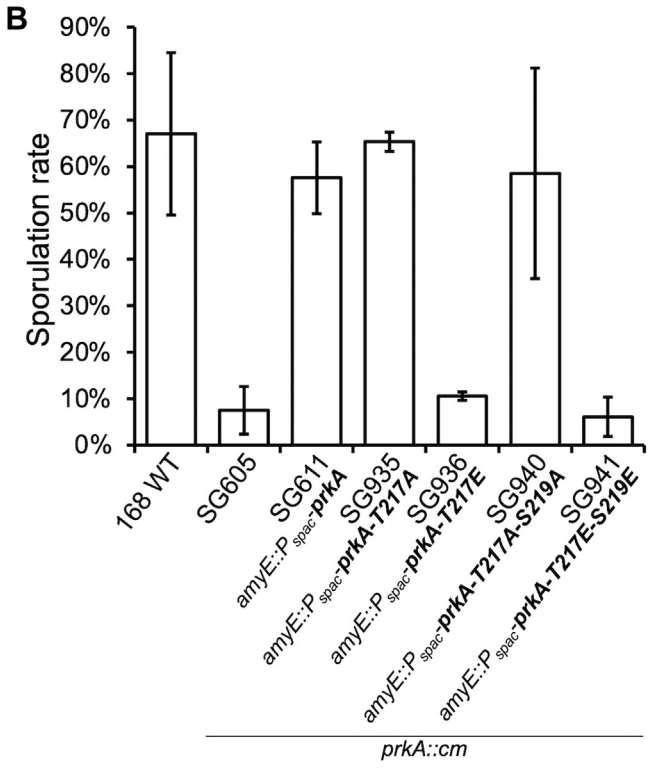

Figure 6. Phosphorylation of PrkA regulates its role in sporulation. *A*, Coomassie-stained SDS-PAGE of α-casein proteolysis by PrkA and mutated PrkA proteins. α-casein proteolytic digestion by PrkA, PrkA-K108A, PrkA-T217A, PrkA-T217D, PrkA-S219A, PrkA-S219D, and PrkA-T217D-S219D was assessed by incubation at 37 °C for 0 (odd-numbered columns) or 21 h (even-numbered columns) in the presence of 1 mM $MgCl_2$ and 1 mM ATP. A control of α-casein alone was run in parallel. *B*, sporulation efficiency of *B. subtilis* strains. Sporulation efficiency (%) was determined from 48 h cultures in DSM as the total number of heat-resistant (80 °C for 20 min) CFUs. The bar graph shows the sporulation rates of the WT, SG605(*prkA::cm*), SG611(*prkA::cm; amyE::Pspac-prkA*), SG935(*prkA::cm; amyE::Pspac-prkA-T217A*), SG936(*prkA::cm; amyE::Pspac-prkA-T217E*), SG940(*prkA::cm; amyE::Pspac-prkA-T217A-S219A*), and SG941(*prkA::cm; amyE::Pspac-prkA-T217E-S219E*) strains. Each experiment was reproduced at least in triplicate, and the standard deviations are represented by the error bars. CFU, colony forming unit; DSM, Difco sporulation medium.

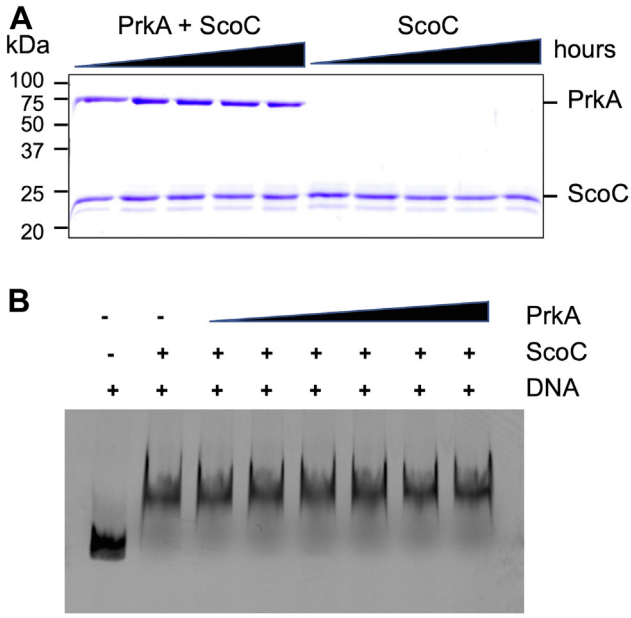

Figure 7. PrkA regulates *B. subtilis* sporulation *via* a ScoC-indirect mechanism. *A*, Coomassie-stained SDS-PAGE of ScoC proteolysis by PrkA. Kinetic of ScoC digestion by PrkA was assessed by incubation at 37 °C for 0, 3, 5, 8, and 25 h in the presence of 1 mM $MgCl_2$ and 1 mM ATP. *B*, electrophoretic mobility shift assay. ScoC (13 μM) binding to cya5-labeled DNA (150 bp of the upstream region of the *epr* gene promoter) was assessed by EMSA in the absence or in the presence of increasing amounts of PrkA (15, 30, 45, 60, 90, and 120 μM) and loaded onto a nondenaturing 4% polyacrylamide gel. EMSA, electrophoretic mobility shift assay.

reduced. The residual protease activity of this mutant protein could be explained by the fact that α-casein has few secondary structures and does not need to be unfolded prior to proteolysis as mentioned in (32). These data may also explain why no difference was observed between heated and unheated α-casein. Hemoglobin, however, does not appear to be a substrate for PrkA, whether folded or not. We have also shown that this ATP-dependent protease activity was required for sporulation of *B. subtilis*.

It is known that Lon proteases degrade their substrates by sequential repetitive rounds of substrate binding, cleavage, release, and rebinding to the proteolytic site, thereby resulting in small, hydrolyzed peptide products (24, 33). When α-casein is incubated in the presence of PrkA and ATP, we can detect intermediate degradation products (Figs. 4*A* and 5*A*), but degradation can also be complete (Fig. 6*A*), suggesting that α-casein is degraded into small peptides. In addition, Lon proteases do not necessarily cleave substrates at a specific peptide consensus sequence (24, 34), and thus, one protease can have several substrates. In the case of PrkA, its native substrates have not yet been identified; they are probably proteins

involved in the initiation of sporulation. Indeed, we observed that the *prkA* mutant strain is not able to form prespores efficiently. The most obvious candidate is the transcriptional regulator ScoC that plays a crucial role in the initiation of sporulation (35) and that was proposed to be regulated by PrkA (11). This assumption has been tested, but ScoC does not appear to be degraded by PrkA. In addition, its DNA binding properties are also not affected by the presence of PrkA. Future work will be necessary to identify the substrate(s) of PrkA, and this is an essential prerequisite to unravel the mechanism by which PrkA regulates the onset of sporulation of *B. subtilis* cells. In this paper, we not only demonstrated that PrkA controlled sporulation through its protease activity but also that this later was regulated *via* phosphorylation by the Ser/Thr kinase PrkC. Indeed, as proteolysis is irreversible, this implies a fine tuning of this activity. Several types of regulation have been described for Lon proteases like direct impact of several effectors (23, 24) or posttranslational modifications of the Lon enzymes themselves or of their protein substrates (25), but more recently, it was also described to be possible *via* phosphorylation (26). Another STPK from *B. subtilis*, YabT, has been described to be involved in sporulation (36) and could also be a good candidate to regulate PrkA by phosphorylation. However, we have tested this possibility, and PrkA does not appear to be phosphorylated under the used conditions (data not shown). It is interesting to note the reverse correlation between *prkC* and *prkA* expression during growth (9) which is in agreement with a negative regulation of PrkA activity by PrkC. Indeed, it is tempting to speculate that when PrkA function is needed (during sporulation), there is less PrkC in the cell and therefore low inhibition of PrkA. However, when spores start to germinate, PrkA function is not necessary anymore, the level of PrkC increases, and PrkC protein is activated by muropeptides (37) which in turn would lead to PrkA inhibition. On the contrary, *prkA* and *yabT* expression are correlated during growth; this may explain why PrkA is not phosphorylated by YabT. It seems therefore that the protease activity of PrkA is specifically regulated by PrkC, thus allowing fine control of sporulation.

Experimental procedures

Plasmids and strains constructions

Standard procedures for molecular cloning and cell transformation of *B. subtilis* and *E. coli* were used. All the strains and plasmids used in this study are listed in Table 1. Primers used in this study are available upon request. Sequencing of PCR-derived DNA fragments in the plasmid constructs was carried out by Eurofins Genomics to ensure error-free amplification.

Fragments containing the *prkA* or the *scoC* genes were amplified by PCR using chromosomal DNA of *B. subtilis* 168 strain, and two specific primers for each amplification then digested with *BamH*I and *Xho*I and cloned into the expression vector pET21a (+) (Novagen). Site-directed mutagenesis using pET21a-*prkA* vector as template was performed to generate the PrkA-K108A, PrkA-T217A, PrkA-T217D, PrkA-T217E, PrkA-S219A, PrkA-S219D, PrkA-S219E, PrkA-T217A-S219A, and PrkA-T217E-S219E modified proteins. The *prkA* gene with its 400 bp upstream promoter region was amplified by PCR using chromosomal DNA of *B. subtilis* 168 strain and two specific primers then digested with *BamH*I and *Eco*RI and cloned into the pAC7 vector. Site-directed mutagenesis using pAC7-*prkA* plasmid as template were performed to generate pAC7-*prkA*-K108A, pAC7-*prkA*-T217A, pAC7-*prkA*-T217E, pAC7-*prkA*-T217A-S219A, and pAC7-*prkA*-T217E-S219E vectors.

Chromosomal DNA of *B. subtilis* 168 strain was used to amplify the flanking sequences of *prkA* (*yhbF* and *yhbH* genes) by PCR with two pairs of primers containing overlapping regions. An isothermal assembly mix (Gibson Assembly Master Mix from NEW ENGLAND BioLabs) containing the two above described fragments and a fragment containing the chloramphenicol resistance gene was then used to generate the whole sequence *yhbF-cm-yhbH* DNA that was used to transform the WT strain to generate the *prkA*-deleted strain SG605. Transformation of SG605 with pAC7-*prkA* and derived mutated plasmids were realized to generate the complementation strains SG611, SG613, SG935, SG936, SG940, and SG941 by insertion at the *amyE* locus. All the *B. subtilis* strains used are listed in Table 1.

Proteins purification

Plasmids (Table 1) overproducing 6His-tagged proteins ScoC and PrkA either in wildtype or mutated forms were used to transform into *E. coli* BL21(DE3). Purification of 6His-tagged recombinant proteins was performed with Ni-NTA resin (Qiagen) as previously described (38). All the proteins were stocked at −80 °C in a buffer containing 20 mM Tris-HCl, pH 7.5, 200 mM NaCl, 15% glycerol. Further purification of PrkA by ion exchange chromatography was carried out using a HiTRAP Q column on AKTA system, and proteins were eluted in 20 mM Tris-HCl, pH 7.5 with a 50 mM to 500 mM NaCl gradient on 15 min at 1 ml/min.

Limited proteolytic digestion

Four micrograms of PrkA were mixed with 40 mM NaCl, 10 mM $MgCl_2$, 10 mM Tris/HCl, pH 7.5 in the absence or in the presence of 1 mM ATP in 50 µl reaction volume. After addition of 0.05 µg of endoproteinase Glu-C (Promega), the reaction mixture was incubated for 0, 15, or 30 min at 37 °C. At each time point, 15 µl of the assay mixtures were collected, and digestion was stopped by adding an equal volume of electrophoresis loading buffer and by heating 5 min at 100 °C before applying the samples onto a 12.5% SDS-PAGE. The gel was then stained with Coomassie Blue reagent.

General growth conditions

Luria-Bertani broth was routinely used for bacterial growth at 37 °C. When necessary, the appropriate antibiotics (ampicillin at 100 µg/ml for *E. coli*, kanamycin at 10 µg/ml and chloramphenicol at 5 µg/ml for *B. subtilis*) were added.

Role of PrkA protease activity in sporulation

Sporulation test

Sporulation was induced by exhaustion in supplemented DSM [8 g/l bacto nutrient broth, 0.1% KCl, 1 mM $MgSO_4$, 22 μg/ml FAC, 1 mM $Ca(NO_3)_2$, 0.01 mM $MnCl_2$, 0.001 mM $FeSO_4$]. Sporulation efficiency was determined from 48 h cultures as the total number of heat-resistant (80 °C for 20 min) colony forming units (CFUs) and compared with WT heat-resistant CFUs (39). Each experiment was reproduced at least in triplicate. Alternatively, the number of spores *versus* the total cells in each 24 or 48 h DSM cultures was determined by counting the spores and cells in images obtained by microscopy on a Zeiss Upright Axio Imager M2 microscope (100×) for four biological replicates of each strain. In order to obtain the mask of cells, the contrast was improved by the following steps: (1) subtract the medial image of each group; (2) remove the background; (3) gaussian unsharp filter; and (4) normalize to maximum intensity by image (FIJI/ImageJ software). The measurements of cells were realized with MicrobeJ plugin (40) of ImageJ software. The statistic treatment was performed with R software. Three cellular types have been highlighted corresponding to the vegetative cells, prespores, and spores morphologies. The classification was based on two cellular features, the maximum intensity and the cell length. The threshold values have been set manually based on intensity *versus* length density scatter graphs. The number of cells belonging to each group from 20 microscopy fields for each strain was then calculated, and the data were collected from four independent biological replicates.

Thermal shift assay

In thin-walled 96-well PCR plates, each well (20 μl) contained 10 μM of PrkA or PrkA-K108A and 2 μl of the fluorescent SYPRO Orange dye solution (Molecular Probes, 5000×, diluted to 100× in water) in 10 mM $MgCl_2$, 25 mM Tris-HCl, pH 7.5, in the presence of increasing concentrations of ATP. The samples were heated from 25 °C to 65 °C in a real-time PCR apparatus CFX96 (Bio-Rad). The fluorescence intensity (Ex/Em = 470/570 nm) of SYPRO Orange was monitored and analyzed from the melt peak using CFX Manager software (Bio-Rad) as indicated in (41). The shift of denaturation temperature (ΔT_m) was plotted against the concentration of ATP. Curve fitting was performed by using Microcal Origin 5.0 software using the following equation $y = \Delta T_m \text{ max} * x^n/((\text{apparent } K_D{}^n + x^n))$, where n is the cooperative binding site. Each experiment was reproduced at least in triplicate.

ATPase activity assay

After determining the appropriate experimental conditions of the ATPase activity assay (Fig. S2), 8 μM of PrkA, PrkA-K108A, or no enzyme (used as negative control) were incubated for 2 min at 37 °C with increasing amounts (0–2 mM) of [γ-^{33}P] ATP (1 μCi) in a 10 μl reaction mixture containing 10 mM Tris/HCl, pH 7.5 and 5 mM $MgCl_2$. The reaction was stopped by addition of 10 μl of 1 M formic acid. Two microliter of each reaction mixture was analyzed by thin layer chromatography using PEI-cellulose F plates (Merck) in 150 mM formic acid and 150 mM LiCl buffer. Plates were then dried and exposed to autoradiography with FLA5100 Typhoon variable-mode imager (Amersham Biosciences). Each experiment was reproduced in triplicate. The amount of Pi released was estimated by using ImageJ software. The specific activity of each protein was calculated in nmol of Pi released/min/nmol of enzyme for each concentration of ATP. The values obtained for the negative control were subtracted from those of the tested proteins. Curve fitting and kinetic parameters determination were performed by using Microcal Origin 5.0 software.

Kinase activity test

Five micrograms of PrkA was incubated for 1 h at 37 °C alone or with 2 μg of myelin basic protein or with 5 μg of *B. subtilis* crude extract from a late stationary phase culture in DSM in a 15 μl reaction mixture containing 10 mM Tris/HCl, pH 7.5, 2.5 mM MgCl2, and 0.5 mM [γ-^{33}P] ATP (1 μCi). The phosphorylation reaction was stopped by adding 5× SDS-sample buffer to the reaction mixtures before 12.5% SDS-PAGE analysis. Gels were then dried and exposed to autoradiography with FLA5100 Typhoon variable-mode imager (Amersham Biosciences).

Protease activity test

0.1 μg/μl of PrkA (or mutated PrkA proteins) was incubated alone or with 0.1 μg/μl of α-casein (or hemoglobin or ScoC) for 0 to 24 h at 37 °C in 40 mM Tris/HCl, pH 7.5, 1 mM $MgCl_2$, and 1 mM ATP. To test PrkA inhibition, addition of 1 mM PMSF or 20 ng of plasmid or 120 ng of cDNA or 0.1 μg/μl of PrkCc (the catalytic domain of PrkC) or inactive PrkCc-K40A were added to the reaction tube. A sample of 15 μl reaction mixture was collected at the appropriate time point, and reaction stopped by adding 5× SDS-sample buffer before a 12.5% SDS-PAGE analysis. To test denatured substrates, α-casein and hemoglobin (from Sigma) were previously heated for 10 min at 85 °C prior proteolytic digestion.

Protein phosphorylation and characterization by mass spectrometry

Five micrograms of PrkA or the mutated PrkA proteins were incubated for 60 min at 37 °C with 5 μg of PrkCc in a 15 μl reaction mixture containing 10 mM Tris/HCl, pH 7.5, 2.5 mM $MgCl_2$, and 0.5 mM [γ-^{33}P] ATP (1 μCi). The phosphorylation reaction was stopped by adding 5× SDS-sample buffer to the reaction mixtures before SDS-PAGE analysis. Gels were then dried and exposed to autoradiography with FLA5100 Typhoon variable-mode imager (Amersham Biosciences). For determination of phosphorylation site(s), PrkA (or mutated PrkA) was phosphorylated *in vitro* by PrkCc as described above with 5 mM ATP. Those proteins (6 μg each, in solution) were digested by trypsin/LysC protease (1/50, w/w)

in 25 mM ammonium bicarbonate, pH 8, overnight. Digested proteins were processed by a desalting step on ZipTip C18 prior injection of 0.6 µg of tryptic peptides onto a nano liquid chromatography Ultimate 3000 (Thermo Scientific) coupled to an ESI-Q-Exactive Plus mass spectrometer (Thermo Scientific) for proteomic analysis, as previously described in (42). Data spectra were processed by Proteome Discoverer software (ThermoFisher, version 2.4.1.15) using the workflow including the Spectrum files ReCalibration,node, the Sequest HT algorithm, and the IMP-ptmRS node specific for better phosphorylation site probability. *B. subtilis* database was extracted from Uniprot (strain 168, TxID 224308 last modified 2021–09–24; 5573 entries) which the natural sequence of PrkA (P39134) was withdrawn, and sequences of recombinant PrkA (or mutated recombinants PrkA) with a C-ter tag –ASSVDKLAAALEHHHHHH were added. Dynamic modifications were searched for oxidation on Met (+15.995) and phosphorylation on Ser/Thr/Tyr (+79.966). Total number of Peptide Spectral Matches (PSM) identifying PrkA, PrkA-T217E and PrkA-S219E were 2883, 3753 and 3757 respectively, allowing 77%, 80% and 85% sequence coverage, respectively.

Electrophoretic mobility shift assay

The DNA probe corresponding to 150 pb in the upstream region of *epr* promoter (27) was generated by PCR using chromosomal DNA of *B. subtilis* 168 strain and specific cya5-labeled primers synthesized from Eurogentec. The reaction mixture between proteins and DNA was performed with a final volume of 20 µl containing 20 mM Tris-HCl, pH 7.5, 1 mM EDTA (pH 8.0), 1 mM DTT, 100 µg/ml BSA, 10 mM $(NH_4)_2SO_4$, 50 mM KCl, 0.2% Tween 20, 0.1 µg poly-L-Lysine, 1 µg sperm salmon, 5 mM ATP, 5 mM $MgCl_2$, 100 nM cya5-labeled DNA probe, 13 µM of ScoC, and increasing amounts (15–120 µM) of PrkA protein. The mixtures were incubated at 37 °C for 15 min and loaded onto a nondenaturing 4% polyacrylamide gel. Electrophoresis was carried out at 95 V in 1× Tris-borate-EDTA buffer. Gels were photographed on a FLA5100 Typhoon variable-mode imager (Amersham Biosciences).

Western blot

The cells were grown at 37 °C in 5 ml of DSM for 8 h then centrifuged for 10 min at 4000 rpm at 4 °C. Cell pellets were resuspended in 1/10th volume of lysis buffer containing 10 mM Tris-HCl, pH 8.0, 150 mM NaCl, 1 mM DTT, 1 mM PMSF, 25 U ml^{-1} benzonase, and 10 mg ml^{-1} lyzozyme. Extracts were incubated for 10 min on ice, then heated at 100 °C for 10 min. Samples were run on a 12.5% SDS-PAGE and transferred to hybond-ECL membrane by electroblotting. The membrane was blocked with PBS-Tween (0.05%) solution containing 5% milk powder (w/v) for 3 h at room temperature with shaking, then incubated with anti-PrkA antibodies diluted to $1/1000^{th}$ overnight at 4 °C. After three washes, the secondary antibody, a peroxidase-conjugated Goat anti-Rabbit (Thermo scientific) antibody, used at $1/2000^{th}$ dilution for 1 h. After three washes, the membrane was incubated with ECL advanced reagents (GE Healthcare) and scanned for chemiluminescence with an ImageQuant LAS4000 (GE Healthcare).

Data availability

All data are contained within the article except primers sequences available upon request. The mass spectrometry proteomics data have been deposited to the ProteomeXchange Consortium *via* the PRIDE (43) partner repository with the dataset identifier PXD032931.

Supporting information—This article contains supporting information (44, 45).

Acknowledgments—We thank Pascal Mansuelle from The Proteomics Platform from the Institut de Microbiologie de la Méditerranée (CNRS, FR3479) which is part of the proteomic network « Marseille Protéomique » (MaP) IBISA and Aix-Marseille Université -labeled for his expertise and technical assistance in mass spectrometry analysis. We thank Etienne Maisonneuve from LCB, CNRS—Marseille for his help with ion exchange and gel filtration purifications. We also thank Jean Michel Jault from IBCP, CNRS—Lyon for helpful discussion.

Author contributions—F. P. and A. G. conceptualization; A. Z. and R. L. investigation; F. P. and A. G. writing original draft; F. P., L. E., and A. Z. methodology; F. P. and A. G. supervision; F. P. writing review and editing.

Funding and additional information—This research was supported by the CNRS and Aix-Marseille University.

Conflict of interest—The authors declare that they have no conflicts of interest with the contents of this article.

Abbreviations—The abbreviations used are: AAA+, ATPases associated with diverse cellular activities; CFU, colony forming unit; DSM, Difco sporulation medium; PMSF, phenylmethylsulfonyl fluoride; STPK, Ser/Thr protein kinases.

References

1. Stragier, P., and Losick, R. (1996) Molecular genetics of sporulation in *Bacillus subtilis*. *Annu. Rev. Genet.* **30**, 297–341
2. Nicholson, W. L., Munakata, N., Horneck, G., Melosh, H. J., and Setlow, P. (2000) Resistance of Bacillus endospores to extreme terrestrial and extraterrestrial environments. *Microbiol. Mol. Biol. Rev.* **64**, 548–572
3. Setlow, P. (2003) Spore germination. *Curr. Opin. Microbiol.* **6**, 550–556
4. Errington, J. (2003) Regulation of endospore formation in *Bacillus subtilis*. *Nat. Rev. Microbiol.* **1**, 117–126
5. Piggot, P. J., and Hilbert, D. W. (2004) Sporulation of *Bacillus subtilis*. *Curr. Opin. Microbiol.* **7**, 579–586
6. Burbulys, D., Trach, K. A., and Hoch, J. A. (1991) Initiation of sporulation in *B. subtilis* is controlled by a multicomponent phosphorelay. *Cell* **64**, 545–552
7. Molle, V., Fujita, M., Jensen, S. T., Eichenberger, P., González-Pastor, J. E., Liu, J. S., *et al.* (2003) The Spo0A regulon of *Bacillus subtilis*. *Mol. Microbiol.* **50**, 1683–1701
8. Setlow, P. (2014) Germination of spores of Bacillus species: what we know and do not know. *J. Bacteriol.* **196**, 1297–1305

9. Pompeo, F., Foulquier, E., and Galinier, A. (2016) Impact of serine/threonine protein kinases on the regulation of sporulation in *Bacillus subtilis*. *Front. Microbiol.* **7**, 568
10. Eichenberger, P., Jensen, S. T., Conlon, E. M., van Ooij, C., Silvaggi, J., González-Pastor, J. E., *et al.* (2003) The sigmaE regulon and the identification of additional sporulation genes in *Bacillus subtilis*. *J. Mol. Biol.* **327**, 945–972
11. Yan, J., Zou, W., Fang, J., Huang, X., Gao, F., He, Z., *et al.* (2015) Eukaryote-like Ser/Thr protein kinase PrkA modulates sporulation via regulating the transcriptional factor σ(K) in *Bacillus subtilis*. *Front. Microbiol.* **6**, 382
12. Fischer, C., Geourjon, C., Bourson, C., and Deutscher, J. (1996) Cloning and characterization of the *Bacillus subtilis prkA* gene encoding a novel serine protein kinase. *Gene* **168**, 55–60
13. Figueira, R., Brown, D. R., Ferreira, D., Eldridge, M. J., Burchell, L., Pan, Z., *et al.* (2015) Adaptation to sustained nitrogen starvation by *Escherichia coli* requires the eukaryote-like serine/threonine kinase YeaG. *Sci. Rep.* **5**, 17524
14. Tagourti, J., Landoulsi, A., and Richarme, G. (2008) Cloning, expression, purification and characterization of the stress kinase YeaG from *Escherichia coli*. *Protein Expr. Purif.* **59**, 79–85
15. Sultan, A., Jers, C., Ganief, T. A., Shi, L., Senissar, M., Køhler, J. B., *et al.* (2021) Phosphoproteome study of Escherichia coli devoid of Ser/Thr kinase YeaG during the metabolic shift from glucose to malate. *Front. Microbiol.* **12**, 657562
16. Hlavácek, O., and Váchová, L. (2002) ATP-dependent proteinases in bacteria. *Folia Microbiol. (Praha)* **47**, 203–212
17. Elsholz, A. K. W., Birk, M. S., Charpentier, E., and Turgay, K. (2017) Functional diversity of AAA+ protease complexes in *Bacillus subtilis*. *Front. Mol. Biosci.* **4**, 44
18. Mahmoud, S. A., and Chien, P. (2018) Regulated proteolysis in bacteria. *Annu. Rev. Biochem.* **87**, 677–696
19. Tsilibaris, V., Maenhaut-Michel, G., and Van Melderen, L. (2006) Biological roles of the Lon ATP-dependent protease. *Res. Microbiol.* **157**, 701–713
20. Walker, J. E., Saraste, M., Runswick, M. J., and Gay, N. J. (1982) Distantly related sequences in the alpha- and beta-subunits of ATP synthase, myosin, kinases and other ATP-requiring enzymes and a common nucleotide binding fold. *EMBO J.* **1**, 945–951
21. Saraste, M., Sibbald, P. R., and Wittinghofer, A. (1990) The P-loop–a common motif in ATP- and GTP-binding proteins. *Trends Biochem. Sci.* **15**, 430–434
22. Madec, E., Laszkiewicz, A., Iwanicki, A., Obuchowski, M., and Seror, S. (2002) Characterization of a membrane-linked Ser/Thr protein kinase in *Bacillus subtilis*, implicated in developmental processes. *Mol. Microbiol.* **46**, 571–586
23. Karlowicz, A., Wegrzyn, K., Gross, M., Kaczynska, D., Ropelewska, M., Siemiątkowska, M., *et al.* (2017) Defining the crucial domain and amino acid residues in bacterial Lon protease for DNA binding and processing of DNA-interacting substrates. *J. Biol. Chem.* **292**, 7507–7518
24. Lee, I., and Suzuki, C. K. (2008) Functional mechanics of the ATP-dependent Lon protease- lessons from endogenous protein and synthetic peptide substrates. *Biochim. Biophys. Acta* **1784**, 727–735
25. Władyka, B., and Pustelny, K. (2008) Regulation of bacterial protease activity. *Cell. Mol. Biol. Lett.* **13**, 212–229
26. Zhou, X., Teper, D., Andrade, M. O., Zhang, T., Chen, S., Song, W. Y., *et al.* (2018) A phosphorylation switch on Lon protease regulates bacterial type III secretion system in host. *mBio* **9**, e02146-17
27. Kodgire, P., Dixit, M., and Rao, K. K. (2006) ScoC and SinR negatively regulate epr by corepression in *Bacillus subtilis*. *J. Bacteriol.* **188**, 6425–6428
28. Hammarén, H. M., Virtanen, A. T., and Silvennoinen, O. (2015) Nucleotide-binding mechanisms in pseudokinases. *Biosci. Rep.* **36**, e00282
29. Lisa, M. N., Wagner, T., Alexandre, M., Barilone, N., Raynal, B., Alzari, P. M., *et al.* (2017) The crystal structure of PknI from *Mycobacterium tuberculosis* shows an inactive, pseudokinase-like conformation. *FEBS J.* **284**, 602–614
30. Rule, C. S., Patrick, M., and Sandkvist, M. (2016) Measuring in vitro ATPase activity for enzymatic characterization. *J. Vis. Exp.* https://doi.org/10.3791/54305
31. Bartolommei, G., Moncelli, M. R., and Tadini-Buoninsegni, F. (2013) A method to measure hydrolytic activity of adenosinetriphosphatases (ATPases). *PLoS One* **8**, e58615
32. Fukui, T., Eguchi, T., Atomi, H., and Imanaka, T. (2002) A membrane-bound archaeal Lon protease displays ATP-independent proteolytic activity towards unfolded proteins and ATP-dependent activity for folded proteins. *J. Bacteriol.* **184**, 3689–3698
33. Mikita, N., Cheng, I., Fishovitz, J., Huang, J., and Lee, I. (2013) Processive degradation of unstructured protein by *Escherichia coli* Lon occurs via the slow, sequential delivery of multiple scissile sites followed by rapid and synchronized peptide bond cleavage events. *Biochemistry* **52**, 5629–5644
34. Ondrovicová, G., Liu, T., Singh, K., Tian, B., Li, H., Gakh, O., *et al.* (2005) Cleavage site selection within a folded substrate by the ATP-dependent Lon protease. *J. Biol. Chem.* **280**, 25103–25110
35. Koide, A., Perego, M., and Hoch, J. A. (1999) ScoC regulates peptide transport and sporulation initiation in *Bacillus subtilis*. *J. Bacteriol.* **181**, 4114–4117
36. Bidnenko, V., Shi, L., Kobir, A., Ventroux, M., Pigeonneau, N., Henry, C., *et al.* (2013) *Bacillus subtilis* serine/threonine protein kinase YabT is involved in spore development via phosphorylation of a bacterial recombinase. *Mol. Microbiol.* **88**, 921–935
37. Pompeo, F., Byrne, D., Mengin-Lecreulx, D., and Galinier, A. (2018) Dual regulation of activity and intracellular localization of the PASTA kinase PrkC during *Bacillus subtilis* growth. *Sci. Rep.* **8**, 1660
38. Galinier, A., Haiech, J., Kilhoffer, M. C., Jaquinod, M., Stulke, J., Deutscher, J., *et al.* (1997) The *Bacillus subtilis crh* gene encodes a HPr-like protein involved in carbon catabolite repression. *Proc. Natl. Acad. Sci. U. S. A.* **94**, 8439–8444
39. Schaeffer, P., Millet, J., and Aubert, J. P. (1965) Catabolic repression of bacterial sporulation. *Proc. Natl. Acad. Sci. U. S. A.* **54**, 704–711
40. Ducret, A., Quardokus, E. M., and Brun, Y. V. (2016) MicrobeJ, a tool for high throughput bacterial cell detection and quantitative analysis. *Nat. Microbiol.* **1**, 16077
41. Foulquier, E., and Galinier, A. (2017) YvcK, a protein required for cell wall integrity and optimal carbon source utilization, binds uridine diphosphate-sugars. *Sci. Rep.* **7**, 4139
42. Zhang, Y., Launay, H., Schramm, A., Lebrun, R., and Gontero, B. (2018) Exploring intrinsically disordered proteins in Chlamydomonas reinhardtii. *Sci. Rep.* **8**, 6805
43. Perez-Riverol, Y., Bai, J., Bandla, C., García-Seisdedos, D., Hewapathirana, S., Kamatchinathan, S., *et al.* (2022) The PRIDE database resources in 2022: a hub for mass spectrometry-based proteomics evidences. *Nucleic Acids Res.* **50**, D543–D552
44. Corpet, F. (1988) Multiple sequence alignment with hierarchical clustering. *Nucleic Acids Res.* **16**, 10881–10890
45. Combet, C., Blanchet, C., Geourjon, C., and Deléage, G. (2000) NPS@: network protein sequence analysis. *Trends Biochem. Sci.* **25**, 147–150